Pergamon

Int. J. Heat Mass Transfer. Vol. 39, No. 11, pp. 2231–2241, 1996
Copyright © 1996 Elsevier Science Ltd
Printed in Great Britain. All rights reserved
0017-9310/96 $15.00 + 0.00

0010-9310(95)00315-0

Heat transfer across a vertical wall separating two fluids at different temperatures

C. TREVIÑO
Facultad de Ciencias, UNAM, México

F. MÉNDEZ
Facultad de Ingeniería, UNAM, México

and

F. J. HIGUERA
ETS Ingenieros Aeronáuticos, UPM, Madrid, Spain

(*Received* 10 *March* 1995 *and in final form* 23 *August* 1995)

Abstract—In this paper we study the conjugate heat transfer across a vertical wall separating two fluids at different temperatures. We present a classification of the solutions of the problem in terms of two main parameters; ε, the ratio of thickness to height of the wall and α, measuring the ratio of the thermal resistance of one of the boundary layers to the thermal resistance of the wall. Numerical and asymptotic solutions are presented for all possible values of α. We show that a maximum average Nusselt number or non-dimensional overall heat flux is attained for values of α much smaller than one, but still large compared with ε^2. Copyright © 1996 Elsevier Science Ltd.

1. INTRODUCTION

The importance of heat transfer phenomena associated with natural convection in boundary layer flows is well known. Due to its fundamental and practical importance, the conjugate coupling heat transfer between two counter-flowing laminar natural convection flows separated by a vertical plate has received particular attention, and different authors have developed a variety of approaches aimed at understanding the interplay of the physical mechanisms involved. Various conjugate heat transfer configurations have been studied since the 1970s using different approximations to deal with the difficulties associated with the simultaneous solution of the flow and thermal boundary layers and the longitudinal and transversal heat conduction in the solid. However, despite the considerable effort invested, the theoretical and experimental results existing in the literature do not yet provide a complete solution of this important problem, which has a bearing on many practical applications, particularly those related to energy conservation in buildings.

The first works on natural convection coupled with conduction considered surfaces with specified heat flux or temperature distributions. Thus, Kelleher and Yang [1] and Lock and Gunn [2] showed that the temperature distribution on a plate is strongly influenced by the interaction between adjacent boundary layers. However, *a priori* specification of temperature or heat transfer distribution at the wall represents a serious shortcoming of these analyses. Lock and Ko [3] introduced a similarity transformation recasting the governing equations into a form suitable for conventional finite difference techniques. They recognized the effect of longitudinal heat conduction in the wall and pointed out that its thermal conductivity may be high enough to render this effect important in many practical cases. Anderson and Bejan [4] presented the first analytical treatment of the problem of counter-flowing free convection boundary layers separated by a vertical plate, using a modified Oseen technique. They considered the contribution of the transversal heat conduction in the plate, but neglected the longitudinal conduction. Using the same methodological procedure, Anderson and Bejan [5] studied theoretically and experimentally the heat transfer through a vertical wall surrounded by thermally-stratified fluids. Viskanta and Lankford [6] applied the superposition technique developed by Churchill and Ozoe [7] and concluded that, for ordinary fluids (liquid metals excepted), the thermal interaction between two laminar convection systems separated by a wall is only moderate. However, they also suggested that further investigations should be carried out for cases where the effect of longitudinal wall conduction is significant. Recently, Sakakibara *et al.* [8] analyzed numerically the same coupled problem, concluding that effectively longitudinal heat conduction in the wall is important when the plate is thick and has a high

NOMENCLATURE

C_{pi}	specific heat of fluid i	β	ratio of boundary layer thermal resistances defined in equation (3)
g	gravity acceleration		
h	thickness of the plate		
L	length of the plate	β_i	thermal expansion coefficient of fluid i
$\overline{Nu}$	Nusselt number defined in equation (25)	ε	plate aspect ratio
Pr_i	Prandtl number of fluid i, $Pr_i = \nu_i \rho_i C_{pi}/\lambda_i$	ψ_i	stream function for fluid i
		λ_i	thermal conductivity of fluid i
q_i	heat flux from fluid i to the wall	λ_w	thermal conductivity of the plate
Ra_i	Rayleigh number of fluid i		
$T_{i\infty}$	temperature of the fluid i far from the plate	ν_i	kinematic coefficient of viscosity of fluid i
x, y	Cartesian coordinates, longitudinal and transversal, respectively.	ρ_i	density of fluid i
		θ_i	nondimensional temperature of fluid i defined in equations (15) and (16)
Greek symbols			
α	heat conduction parameter defined in equation (6)	θ_w	nondimensional temperature of the plate defined in equation (14).

thermal conductivity. These authors indicated that the use of similarity variables to reduce the governing equations in the numerical calculations is too complex for this class of problems. Córdova and Treviño [9] used multiple-scales perturbation techniques to analyze the cooling of a vertical thin plate caused by a free convective flow; they showed that, owing to the finite thermal conductivity of the plate, a longitudinal temperature gradient appears that prevents a similarity solution of the free boundary layer flow. Indeed, the mathematical problem is elliptic rather than parabolic, even in the high Rayleigh number limit.

In the present paper, a theoretical analysis is conducted of the heat transfer process between two fluids at different temperatures separated by a vertical wall. In this configuration we have two counter-flowing boundary layers, rendering the problem elliptic even in the absence of longitudinal heat conduction (whose effect is also included in this work). The conservation equations reduce to a system of five partial differential equations with five parameters: the Prandtl numbers of the fluids, Pr_I and Pr_{II}, the heat conduction parameter α, which corresponds to the ratio of heat conducted by the plate to the heat convected from the hot fluid to the plate, ε, the aspect ratio of the plate, and finally the parameter, β, relating the two boundary layer thicknesses. For reference, we note here the correspondence $M = \beta$ and $P = \varepsilon^2/\alpha$ with the parameters M and P of Viskanta and Lankford [6].

2. ORDERS OF MAGNITUDE AND FORMULATION

The physical model under study is shown in Fig. 1. A thin vertical plate of length L and thickness h separates two fluids with different temperatures; the fluid at the left of the plate (denoted by the subscript I) is at a temperature $T_{I\infty}$ and the fluid at the right (denoted by II) is at a temperature $T_{II\infty} < T_{I\infty}$. The thermal conductivity of the solid enables heat conduction both across and along the plate, whereas two counter-flowing viscous, nonisothermal natural convection boundary layers develop in the fluids owing to the temperature or the corresponding density differences. We shall be interested in steady-state solutions, and in particular in the temperature distribution of the plate and the overall rate of heat transfer.

For fluids with Prandtl numbers of order unity or larger, the characteristic thicknesses of both thermal boundary layers are

$$\delta_I \sim L\left(\frac{\Delta T}{Ra_I \Delta T_I}\right)^{1/4} \quad \text{and} \quad \delta_{II} \sim L\left(\frac{\Delta T}{Ra_{II} \Delta T_{II}}\right)^{1/4},$$

where $Ra_i \gg 1$ are the Rayleigh numbers defined by

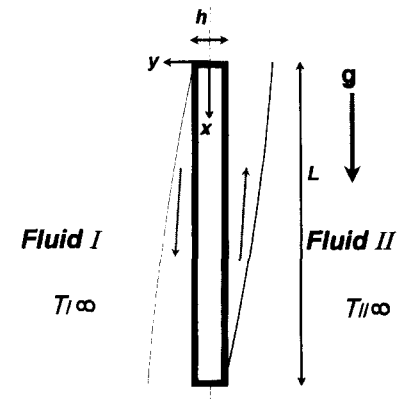

Fig. 1. Schematic diagram of the physical configuration studied.

$$Ra_i = \frac{g\beta_i \Delta T L^3 \rho_i C_{pi}}{\nu_i \lambda_i}, \quad (1)$$

$\Delta T = T_{\mathrm{I}\infty} - T_{\mathrm{II}\infty}$, and ΔT_i ($i = \mathrm{I}, \mathrm{II}$) are the characteristic temperature changes in the fluids, determined below. Here, g is the acceleration of gravity; ρ_i, C_{pi}, β_i, ν_i and λ_i are the density, specific heat (at constant pressure for a gas), coefficient of thermal expansion, kinematic coefficient of viscosity and thermal conductivity of fluid i, respectively.

The orders of magnitude of the heat fluxes across the boundary layers in the fluids are

$$q_{\mathrm{I}} \sim \frac{\lambda_{\mathrm{I}} \Delta T_{\mathrm{I}}^{5/4} Ra_{\mathrm{I}}^{1/4}}{L \Delta T^{1/4}} \quad \text{and} \quad q_{\mathrm{II}} \sim \frac{\lambda_{\mathrm{II}} \Delta T_{\mathrm{II}}^{5/4} Ra_{\mathrm{II}}^{1/4}}{L \Delta T^{1/4}}, \quad (2)$$

and by equating these two estimates we obtain the following relationship between the characteristic temperature changes in both fluids:

$$\frac{\Delta T_{\mathrm{II}}}{\Delta T_{\mathrm{I}}} \sim \beta^{4/5}, \quad \text{with } \beta = \frac{\lambda_{\mathrm{I}}}{\lambda_{\mathrm{II}}} \left(\frac{Ra_{\mathrm{I}}}{Ra_{\mathrm{II}}} \right)^{1/4}. \quad (3)$$

In addition, the transversal heat flux across the wall must be of the same order of magnitude as the heat fluxes in the fluids; that is

$$\frac{\lambda_{\mathrm{I}} \Delta T_{\mathrm{I}}^{5/4} Ra_{\mathrm{I}}^{1/4}}{L \Delta T^{1/4}} \sim \frac{\lambda_{\mathrm{w}} \Delta T_{\mathrm{w}}}{h}, \quad (4)$$

where λ_{w} is the thermal conductivity of the plate and ΔT_{w} is the characteristic temperature change across the plate. Relation (4) can be recast in the form

$$\Delta T_{\mathrm{w}} \sim \frac{\varepsilon^2}{\alpha} \frac{\Delta T_{\mathrm{I}}^{5/4}}{\Delta T^{1/4}}, \quad (5)$$

where

$$\varepsilon = h/L \ll 1 \quad \text{and} \quad \alpha = \frac{\lambda_{\mathrm{w}}}{\lambda_{\mathrm{I}}} \frac{h}{L} Ra_{\mathrm{I}}^{-1/4}. \quad (6)$$

To see the significance of α/ε^2, we note that $\Delta T_{\mathrm{I}} + \Delta T_{\mathrm{II}} + \Delta T_{\mathrm{w}} = \Delta T$ and use relations (3) and (5) to obtain the following relationship for ΔT_{w}:

$$\left(\frac{\alpha}{\varepsilon^2} \right)^{4/5} (1+\beta^{4/5}) \left(\frac{\Delta T_{\mathrm{w}}}{\Delta T} \right)^{4/5} + \left(\frac{\Delta T_{\mathrm{w}}}{\Delta T} \right) \sim 1. \quad (7)$$

The first term in (7) is much larger than the second for large values of the parameter α/ε^2, giving

$$\frac{\Delta T_{\mathrm{w}}}{\Delta T} \sim \frac{1}{(\alpha/\varepsilon^2)(1+\beta^{4/5})^{5/4}} \ll 1 \quad \text{for} \quad \frac{\alpha}{\varepsilon^2} \gg 1; \quad (8)$$

i.e. the transversal temperature variations in the solid are very small, of order ε^2/α at most, for large values of α/ε^2. On the contrary, for very small values of α/ε^2 (and β bounded), the first term in (7) is much smaller than the second which, along with equation (5), gives

$$\frac{\Delta T_{\mathrm{I}}}{\Delta T} \sim \left(\frac{\alpha}{\varepsilon^2} \right)^{4/5} \ll 1 \quad \text{and} \quad \Delta T_{\mathrm{w}} \simeq \Delta T \quad \text{for} \quad \frac{\alpha}{\varepsilon^2} \ll 1. \quad (9)$$

In this limit most of the transversal temperature drop occurs in the solid.

In order to ascertain the effect of longitudinal heat conduction on the overall heat transfer process, we must compare the heat transfer by conduction along the solid, of order $h(\lambda_{\mathrm{w}} \Delta T_{\mathrm{Lw}}/L)$ (with ΔT_{Lw} denoting the characteristic temperature change along the solid), with the heat transfer from the fluids to the solid, of order $Lq_{\mathrm{I}} \sim L(\lambda_{\mathrm{w}} \Delta T_{\mathrm{w}}/h)$ [using equation (4)]. The ratio of the two is $R \sim \varepsilon^2 \Delta T_{\mathrm{Lw}}/\Delta T_{\mathrm{w}}$ or, using relationship (8),

$$R \sim \alpha(1+\beta^{4/5})^{5/4} \frac{\Delta T_{\mathrm{Lw}}}{\Delta T} \quad \text{for} \quad \frac{\alpha}{\varepsilon^2} \gg 1, \quad (10)$$

which is independent of ε in this limit. Thus the ratio $\Delta T_{\mathrm{Lw}}/\Delta T$ should be of order $1/(\alpha(1+\beta^{4/5})^{5/4})$ for the longitudinal conduction to matter but, since it cannot be larger than one, the effect of longitudinal conduction is negligible (except in small regions close to the edges of the plate; see below) for values of α such that $\alpha \ll 1/(1+\beta^{4/5})^{5/4}$. This result, in turn, justifies the use of (8) to obtain (10), because longitudinal conduction is clearly negligible ($R \ll 1$) before α decreases to become of order ε^2. In the opposite limit, $\alpha(1+\beta^{4/5})^{5/4} \gg 1$, longitudinal conduction is dominant. Since R cannot be large, relation (10) then implies

$$\frac{\Delta T_{\mathrm{Lw}}}{\Delta T} \sim \frac{1}{\alpha(1+\beta^{4/5})^{5/4}} \ll 1 \quad \text{in this limit.} \quad (11)$$

Finally, we write two estimates of the overall heat flux or Nusselt number that will guide us through the analysis that follows. From (4) and (8) or (9), we obtain

$$\frac{qL}{\lambda_{\mathrm{I}} \Delta T} \sim \frac{Ra_{\mathrm{I}}^{1/4}}{(1+\beta^{4/5})^{5/4}} \quad \text{for} \quad \frac{\alpha}{\varepsilon^2} \gg 1 \quad (12)$$

and

$$\frac{qL}{\lambda_{\mathrm{I}} \Delta T} \sim \frac{Ra_{\mathrm{I}}^{1/4} \alpha}{\varepsilon^2} \quad \text{for} \quad \frac{\alpha}{\varepsilon^2} = O(1). \quad (13)$$

Therefore the non-dimensional overall heat flux or overall Nusselt number does not depend on α or ε for large values of α/ε^2, whereas it decreases with α/ε^2 for values of α/ε^2 of order unity.

Let us introduce the nondimensional variables

$$\chi = \frac{x}{L}, \quad z = \frac{y}{h}, \quad \theta_{\mathrm{w}} = \frac{T_{\mathrm{w}} - T_{\mathrm{II}\infty}}{T_{\mathrm{I}\infty} - T_{\mathrm{II}\infty}} \quad (14)$$

for the solid, where x is the vertical distance along the plate measured from its upper edge and y is the horizontal distance from the middle of the plate; the variables

$$\chi_{\rm I} = \chi, \quad \eta_{\rm I} = \frac{Ra_{\rm I}^{1/4}(y-h/2)}{L\chi_{\rm I}^{1/4}},$$

$$f_{\rm I}(\chi_{\rm I}, \eta_{\rm I}) = \frac{\psi_{\rm I}}{\nu_{\rm I} Ra_{\rm I}^{1/4}\chi_{\rm I}^{3/4}}, \quad \theta_{\rm I} = \frac{T_{\rm I\infty} - T_{\rm I}}{T_{\rm I\infty} - T_{\rm II\infty}} \quad (15)$$

for the downward moving fluid in the boundary layer at the left of the plate; and

$$\chi_{\rm II} = 1-\chi, \quad \eta_{\rm II} = -\frac{Ra_{\rm II}^{1/4}(y+h/2)}{L\chi_{\rm II}^{1/4}},$$

$$f_{\rm II}(\chi_{\rm II}, \eta_{\rm II}) = \frac{\psi_{\rm II}}{\nu_{\rm II} Ra_{\rm II}^{1/4}\chi_{\rm II}^{3/4}}, \quad \theta_{\rm II} = \frac{T_{\rm II} - T_{\rm II\infty}}{T_{\rm I\infty} - T_{\rm II\infty}} \quad (16)$$

for the upward moving fluid in the boundary layer at the right of the plate. Here $f_{\rm I}$ and $f_{\rm II}$ are the scaled stream functions in the respective fluids.

The Laplace equation describing the heat conduction in the solid is

$$\frac{\partial^2\theta_{\rm w}}{\partial\chi^2} + \frac{1}{\varepsilon^2}\frac{\partial^2\theta_{\rm w}}{\partial z^2} = 0, \quad (17)$$

and the boundary conditions at the adiabatic edges of the wall are

$$\left.\frac{\partial\theta_{\rm w}}{\partial\chi}\right|_{\chi=0,1} = 0. \quad (18)$$

At the interfaces solid–fluid ($z = \pm 1/2$), continuity of the temperature and the heat flux gives

$$1-\theta_{\rm I}(\chi_{\rm I}, \eta_{\rm I}=0) = \theta_{\rm w}(\chi, z=1/2)$$

$$\text{and} \quad \left.\frac{\partial\theta_{\rm w}}{\partial z}\right|_{z=1/2} = -\frac{\varepsilon^2}{\alpha}\frac{1}{\chi_{\rm I}^{1/4}}\left.\frac{\partial\theta_{\rm I}}{\partial\eta_{\rm I}}\right|_{\eta_{\rm I}=0} \quad (19)$$

and

$$\theta_{\rm II}(\chi_{\rm II}, \eta_{\rm II}=0) = \theta_{\rm w}(1-\chi, z=-1/2)$$

$$\text{and} \quad \left.\frac{\partial\theta_{\rm w}}{\partial z}\right|_{z=-1/2} = -\frac{\varepsilon^2}{\alpha\beta}\frac{1}{\chi_{\rm II}^{1/4}}\left.\frac{\partial\theta_{\rm II}}{\partial\eta_{\rm II}}\right|_{\eta_{\rm II}=0}. \quad (20)$$

The nondimensional longitudinal momentum and energy equations for both fluids take the form ($i = {\rm I}, {\rm II}$)

$$\frac{\partial^3 f_i}{\partial\eta_i^3} + \theta_i = \frac{1}{Pr_i}\left\{\frac{1}{2}\left(\frac{\partial f_i}{\partial\eta_i}\right)^2 - \tfrac{3}{4}f_i\frac{\partial^2 f_i}{\partial\eta_i^2} + \chi_i\left[\frac{\partial f_i}{\partial\eta_i}\frac{\partial^2 f_i}{\partial\chi_i\partial\eta_i} - \frac{\partial f_i}{\partial\chi_i}\frac{\partial^2 f_i}{\partial\eta_i^2}\right]\right\} \quad (21)$$

$$\frac{\partial^2\theta_i}{\partial\eta_i^2} = -\tfrac{3}{4}f_i\frac{\partial\theta_i}{\partial\eta_i} + \chi_i\left[\frac{\partial f_i}{\partial\eta_i}\frac{\partial\theta_i}{\partial\chi_i} - \frac{\partial f_i}{\partial\chi_i}\frac{\partial\theta_i}{\partial\eta_i}\right] \quad (22)$$

with the boundary conditions

$$f_i = \frac{\partial f_i}{\partial\eta_i} = 0 \quad \text{at} \quad \eta_i = 0, \quad (23)$$

$$\theta_i = \frac{\partial f_i}{\partial\eta_i} = 0 \quad \text{for} \quad \eta_i \to \infty, \quad (24)$$

in addition to the conditions (19) and (20). The initial conditions for equations (21) and (22) at $\chi_{\rm I} = 0$ and $\chi_{\rm II} = 0$ are the well known self-similar solutions of these equations without the terms proportional to χ_i. The solution of the problem (17)–(24), for which some numerical results have been presented in ref. [8], should provide

$$\theta_{\rm w} = F(\alpha, \beta, \varepsilon, Pr_{\rm I}, Pr_{\rm II}, \chi, z)$$

and the overall Nusselt number

$$\overline{Nu} = \frac{\bar{q}L}{\lambda_{\rm I}\Delta T}, \quad (25)$$

where

$$\bar{q} = -\frac{\lambda_{\rm I} Ra_{\rm I}^{1/4}\Delta T}{L}\int_0^1 \left.\frac{\partial\theta_{\rm I}}{\partial\eta_{\rm I}}\right|_0 \frac{{\rm d}\chi_{\rm I}}{\chi_{\rm I}^{1/4}}$$

$$= -\frac{\lambda_{\rm II} Ra_{\rm II}^{1/4}\Delta T}{L}\int_0^1 \left.\frac{\partial\theta_{\rm II}}{\partial\eta_{\rm II}}\right|_0 \frac{{\rm d}\chi_{\rm II}}{\chi_{\rm II}^{1/4}}. \quad (26)$$

We notice here for reference that the overall heat flux $\bar{q}$ from fluid I to the wall coincides with the heat flux from the wall to fluid II, owing to the adiabatic conditions at the edges of the plate.

In the remainder of this paper we classify the solutions according to the value of α, taking advantage of the fact that ε^2 is very small in general. For large values of α/ε^2 the transverse temperature variations in the plate are very small and the plate temperature can be assumed to be a function of the longitudinal coordinate χ only. (It is to be noted that neglecting the transverse temperature variations does not mean neglecting the transverse temperature gradient, which is always retained in the analysis.) In Section 3 we present numerical solutions of this problem for $\alpha = O(1)$ and analyze the limits of large and small values of α using asymptotic and numerical techniques. The temperature variation across the plate must be taken into account for α/ε^2 of order unity, but the longitudinal heat conduction is then negligible, except in small regions close to the edges of the plate. Numerical solutions for this case are presented in Section 4, and the asymptotic limits of large and small values of α/ε^2 are analyzed.

3. CASE $\varepsilon \to 0$ WITH α FINITE

In this case the non-dimensional transverse temperature variations in the plate are very small, of order

ε^2/α. Integrating the energy equation (17) across the solid and applying the boundary conditions (19) and (20), we obtain

$$\alpha\frac{d^2\theta_w}{d\chi^2}=\frac{1}{\chi^{1/4}}\left.\frac{\partial\theta_I}{\partial\eta_I}\right|_{\eta_I=0}-\frac{1}{\beta(1-\chi)^{1/4}}\left.\frac{\partial\theta_{II}}{\partial\eta_{II}}\right|_{\eta_{II}=0}, \tag{27}$$

with

$$1-\theta_I(\chi_I,\eta_I=0)=\theta_{II}(1-\chi_{II},\eta_{II}=0)=\theta_w(\chi). \tag{28}$$

The problem (18), (21)–(24), (27) and (28) has been solved numerically. For this purpose, the nondimensional wall temperature θ_w was computed from equations (27) and (18) by means of a pseudo-transient procedure that amounts to writing equation (27) in the form

$$\frac{\partial\theta_w}{\partial\tau}=\alpha\chi^{1/4}(1-\chi)^{1/4}\frac{\partial^2\theta_w}{\partial\chi^2}-(1-\chi)^{1/4}\left.\frac{\partial\theta_I}{\partial\eta_I}\right|_0+\left.\frac{\chi^{1/4}}{\beta}\frac{\partial\theta_{II}}{\partial\eta_{II}}\right|_0,$$

and marching in the artificial time τ until a steady state is attained. The nondimensional heat fluxes $(\partial\theta_i/\partial\eta_i)_0$ were obtained at each time step, in terms of the instantaneous wall temperature distribution, by solving the boundary layer equations with a standard finite difference method.

3.1. *Asymptotic limit* $\alpha\to\infty$

The asymptotic solution of the problem for large values of α is important because it is applicable to many practical cases of metallic plates in air or water. For $\alpha\gg1$ the nondimensional temperature of the plate changes very little in the longitudinal direction. In fact this change is of order α^{-1} as shown by the order of magnitude estimate (11). Neglecting such a small quantity in the first approximation, the temperature of the plate can be approximated by an unknown constant θ_{w0}, and the flows in the boundary layers are then self-similar, of the form

$$f_I=(1-\theta_{w0})^{1/4}g[(1-\theta_{w0})^{1/4}\eta_I,Pr_I],$$
$$\theta_I=(1-\theta_{w0})\phi[(1-\theta_{w0})^{1/4}\eta_I,Pr_I], \tag{29}$$

and

$$f_{II}=\theta_{w0}^{1/4}g[\theta_{w0}^{1/4}\eta_{II},Pr_{II}],\quad \theta_{II}=\theta_{w0}\phi[\theta_{w0}^{1/4}\eta_{II},Pr_{II}], \tag{30}$$

where $g(\xi,Pr)$ and $\phi(\xi,Pr)$ are the solution of the classical problem

$$\frac{d^3g}{d\xi^3}+\phi=\frac{1}{Pr}\left\{\frac{1}{2}\left(\frac{dg}{d\xi}\right)^2-\frac{3}{4}g\frac{d^2g}{d\xi^2}\right\}, \tag{31}$$

$$\frac{d^2\phi}{d\xi^2}+\tfrac{3}{4}g\frac{d\phi}{d\xi}=0, \tag{32}$$

$$g(0)=\left.\frac{dg}{d\xi}\right|_{\xi=0}=\phi(0)-1=0,$$

$$\text{and}\quad \left.\frac{dg}{d\xi}\right|_{\xi\to\infty}=\phi(\infty)=0, \tag{33}$$

and use has been made of the invariance of equations (31) and (32) under the group of transformations $g\Rightarrow B^{1/4}g$, $\phi\Rightarrow B\phi$, and $\xi\Rightarrow B^{-1/4}\xi$, with B arbitrary.

The solution of equations (31)–(33) can be found elsewhere (Kays and Crawford, [10]). In particular, the nondimensional temperature gradient at the wall is given by the very good correlation

$$\left.\frac{d\phi}{d\xi}\right|_{\xi=0}=-G(Pr_i)\approx-\frac{3}{4}\left[\frac{2Pr_i/5}{1+2Pr_i^{1/2}+2Pr_i}\right]^{1/4}. \tag{34}$$

The unknown θ_{w0} can be found by using equations (29), (30) and (34) to evaluate the right hand side of equation (27) and then integrating this equation over χ with the boundary conditions (18). The result is

$$\theta_{w0}=\frac{1}{1+\left(\dfrac{G_{II}}{\beta G_I}\right)^{4/5}} \tag{35}$$

where $G_i=G(Pr_i)$. Assuming that the Prandtl numbers of the two fluids are of the same order, we can see that $\theta_{w0}\to1$ for large values of β and $\theta_{w0}\to0$ for small values of β. The two limits correspond to the cases where the thermal resistance of the very thin boundary layer of fluid I or II, respectively, is negligible and the temperature of the plate is very close to $T_{I\infty}$ or to $T_{II\infty}$. In the particular case in which the fluids at both sides of the wall are the same, $\beta=1$ and $\theta_{w0}=1/2$. Once θ_{w0} is known, the total heat transfer rate given by equation (26) and the overall Nusselt number given by equation (25) can be evaluated, giving

$$\overline{Nu}=\tfrac{4}{3}G_I(1-\theta_{w0})^{5/4}Ra_I^{1/4}. \tag{36}$$

This result can be improved by computing the next term in an expansion of the solution in powers of α^{-1}. Such calculation is summarized in the Appendix and gives the correction factor

$$[1+\alpha^{-1}F(Pr_I,Pr_{II},\beta)] \tag{37}$$

for the Nusselt number equation (36), with F given by equation (A13). The resulting approximation turns out to be very good, even for α of order unity.

3.2. *Asymptotic limit* $\alpha\to0$

Taking the limit $\alpha\to0$ in equation (27) we find, as was advanced in Section 2, that the effect of the longitudinal heat conduction in the solid becomes neg-

ligible and the local heat flux from fluid I to the wall equals the heat flux from the wall to fluid II at each point of the wall. Since the second of these fluxes is obviously finite near the upper edge of the wall, so must be the first, requiring that the wall temperature and the temperature of fluid I be of the form $[(1-\theta_w), \theta_I] \sim \chi^{1/5}$. Analogously, $(\theta_w, \theta_{II}) \sim (1-\chi)^{1/5}$ near the lower edge. Appropriate variables to deal with this situation are

$$\tilde{\theta}_w = \frac{\theta_w + \chi - 1}{\chi^{1/5}(1-\chi)^{1.5}},$$

and

$$\tilde{\eta}_i = \frac{Ra_i^{1/4}(-h/2 \pm y)}{L\chi_i^{1/5}},$$

$$\tilde{f}_i(\chi_i, \tilde{\eta}_i) = \frac{\psi_i}{\nu_i Ra_i^{1/4}\chi_i^{4/5}}, \quad \tilde{\theta}_i = \frac{\theta_i}{\chi_i^{1/5}}. \tag{38}$$

Equations (21)–(24) and (28) were rewritten in terms of these variables, whereas equation (27) was replaced by its limiting form

$$\left.\frac{\partial \tilde{\theta}_I}{\partial \tilde{\eta}_I}\right|_{\tilde{\eta}_I = 0} = \frac{1}{\beta}\left.\frac{\partial \tilde{\theta}_{II}}{\partial \tilde{\eta}_{II}}\right|_{\tilde{\eta}_{II} = 0}, \tag{39}$$

and the resulting problem was solved numerically using the same method commented on before, with a term $\partial\tilde{\theta}_w/\partial\tau$ added to the left hand side of equation (39) during the pseudo-transient.

The solution of this problem does not satisfy the adiabatic conditions (18) at the edges of the plate. Evaluating the left hand side of equation (27) with this solution, we find that it is of order $\alpha/\chi^{9/5}$ near the upper edge, becoming of order unity for $\chi \sim \alpha^{5/9}$, where $(1-\theta_w) \sim \alpha^{1/9}$. In this region, and in a similar region around the lower edge, the effect of the longitudinal conduction in the solid is not negligible. Analysis of these regions, which is not presented here, would determine the precise values of the temperatures at the edges.

3.3. *Results*

The wall temperature distribution resulting from the numerical solution of equations (18), (21)–(24), (27) and (28) is plotted in Fig. 2 for $Pr_i = 1$, $\beta = 0.5$ and 1, and different values of α, while Fig. 3 is a sample nondimensional temperature profile in both fluids for $\alpha = 0.1$ and $\beta = Pr_i = 1$. The results of Fig. 2 show a flat temperature distribution for α above about 0.5. For smaller values of α, the temperature of the upper half of the plate begins to approach the temperature of the hot fluid, while the temperature of the lower half of the plate approaches that of the cold fluid. The same trends persist for smaller values of β, but the plate temperatures are lower. For $\alpha \ll 1$ longitudinal heat conduction in the wall becomes negligible, except in small regions close to the edges. Figure 2 also shows

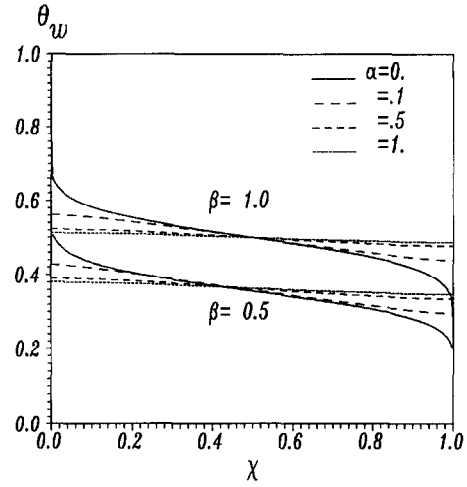

Fig. 2. Non-dimensional wall temperature distribution for several values of α, with $Pr_I = Pr_{II} = 1$ and $\beta = 0.5$ and 1.

the solution in the asymptotic limit $\alpha \to 0$ of Section 3.2.

In Figure 4 we compare the wall temperature distributions from the numerical solution and the two-term asymptotic solution for large values of α. Here we chose $\beta = 1$, $Pr_I = Pr_{II} = 1$, and two different values of α. The difference between the two solutions is rather small for $\alpha = 0.5$, and decreases rapidly with increasing α. For $\alpha < 0.5$ the asymptotic solution overestimates the longitudinal temperature gradients, and pronounced discrepancies can be appreciated for $\alpha = 0.1$.

Figure 5 shows the overall reduced Nusselt number $\overline{Nu}/Ra_I^{1/4}$, computed from the numerical and asymptotic solutions, as a function of α for $\beta = 0.5$ and 1. As can be seen, the asymptotic solution for large α predicts correctly the overall Nusselt number for values of $\alpha \geqslant 0.5$. As was mentioned before, the thermal resistance of fluid II is smaller than that of fluid I when $\beta < 1$. It turns out that a decrease of β leads to

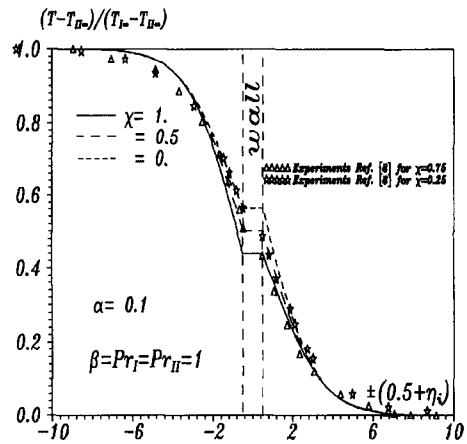

Fig. 3. Nondimensional temperature profiles in both fluids for $\alpha = 0.1$, $\beta = Pr_i = 1$, and different values of χ. Experimental results from ref. [8] for $\chi = 0.25$ and 0.75 are also included.

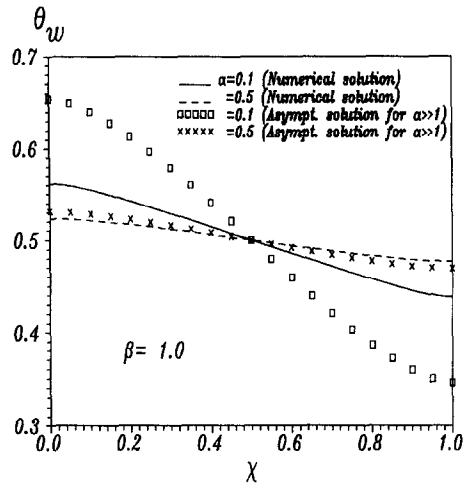

Fig. 4. Comparison of the nondimensional wall temperatures from the numerical solution and the asymptotic solution for large values of α. Displayed distributions correspond to $\alpha = 0.1$ and 0.5, and $\beta = Pr_I = Pr_{II} = 1$.

a Nusselt number larger than for the symmetric case $\beta = 1$. The solutions for $\beta > 1$ can be obtained from those of $\beta < 1$ using the invariance of the problem under the transformation

$$\beta \Rightarrow \frac{1}{\beta}, \quad \alpha \Rightarrow \alpha\beta, \quad \theta_w \Rightarrow 1-\theta_w, \quad \chi \Rightarrow 1-\chi,$$

$$\mathrm{I} \Leftrightarrow \mathrm{II}, \frac{\overline{Nu}}{Ra_i^{1/4}} \Rightarrow \beta \frac{\overline{Nu}}{Ra_i^{1/4}}.$$

Perhaps the most noticeable feature revealed by Fig. 5 is the increase of the overall Nusselt number with decreasing α. To explain this result we may begin recalling that longitudinal heat conduction makes the plate temperature uniform for large values of α, leading to constant temperature differences between the plate and each of the fluids. Then, as α decreases,

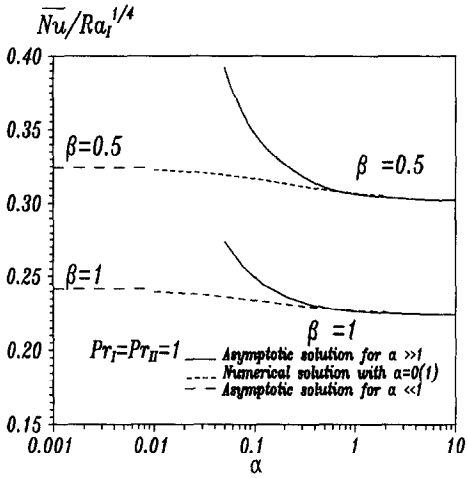

Fig. 5. Overall reduced Nusselt number, $\overline{Nu}/Ra_I^{1/4}$, as a function for α, for $\beta = 0.5$ and 1. Results from the numerical solution (dashed curves) and from the asymptotic solutions for large and small α.

Table 1.

β	1	0.667	0.5	0.4	0.333	0
$(\overline{Nu}/Ra_I^{1/4})_{max}$	0.242	0.291	0.324	0.349	0.367	0.535

longitudinal temperature variations arise in the plate that increase these solid-to-fluid temperature differences in some parts of the plate and decrease them in others. But, since the local heat flux is roughly proportional to the corresponding temperature difference to the power 5/4 (cf. the group of transformations mentioned in the paragraph below equations (31)–(33) and the analysis of the following section), the effect of the former regions offsets that of the latter, resulting in a net increase of the overall heat transfer. Moreover, we'll see in the following section that the temperature drop across the plate reduces the temperature differences between the surfaces of the plate and the fluids when α becomes of order ε^2, and the overall heat flux then decreases with α. Therefore, a maximum overall Nusselt number exists for some α verifying $\varepsilon^2 \ll \alpha \ll 1$. Values of this maximum Nusselt number are given in Table 1 for some values of β.

These results, valid in the asymptotic limit $\varepsilon \to 0$, correspond to the solution of Section 3.2. Values of

$$(\overline{Nu}/Ra_I^{1/4})_{max}$$

for $\beta > 1$ can be obtained from the ones of the table using the transformation commented on before.

4. CASE $\varepsilon \to 0$ WITH α/ε^2 FINITE

In this case the non-dimensional temperature varies linearly across the plate between values $\theta_{wI}(\chi)$ and $\theta_{wII}(\chi)$ at the faces, with $\theta_{wI}(\chi) - \theta_{wII}(\chi) = O(1)$. As in Subsection 3.2, the longitudinal heat conduction can be neglected, except in small regions close to the edges of the plate, and the heat flux from fluid I to the left face of the wall and from the right face to fluid II are locally equal to each other, and equal to the heat flux across the solid. Also as in that case, the facts that the heat flux in fluid II is finite at the upper edge and the heat flux in fluid I is finite at the lower edge imply $[(1-\theta_w), \theta_I] \sim \chi^{1/5}$ for χ small and $(\theta_w, \theta_{II}) \sim (1-\chi)^{1/5}$ for $(1-\chi)$ small. The variables (38) are still appropriate for the fluids, and the conditions that the three heat fluxes referred to before be equal are

$$\left.\frac{\partial\tilde{\theta}_I}{\partial\tilde{\eta}_I}\right|_{\tilde{\eta}_I=0} = \frac{\alpha}{\varepsilon^2}(\theta_{wII}(\chi) - \theta_{wI}(\chi)) = \frac{1}{\beta}\left.\frac{\partial\tilde{\theta}_{II}}{\partial\tilde{\eta}_{II}}\right|_{\tilde{\eta}_{II}=0}. \tag{40}$$

For the pseudo-transient numerical treatment, this equation was written as the pair of equations

$$\frac{\partial\tilde{\theta}_{wI}}{\partial\tau} = \left.\frac{\partial\tilde{\theta}_I}{\partial\tilde{\eta}_I}\right|_0 - \frac{\alpha}{\varepsilon^2}(\theta_{wII} - \theta_{wI})$$

and

$$\frac{\partial \tilde{\theta}_{wII}}{\partial \tau} = \frac{1}{\beta}\left.\frac{\partial \tilde{\theta}_{II}}{\partial \tilde{\eta}_{II}}\right|_0 - \frac{\alpha}{\varepsilon^2}(\theta_{wII} - \theta_{wI}),$$

which amounts to assigning a fictitious thermal inertia to the interfaces.

The regions around the edges where longitudinal conduction matters are now of length $O(\varepsilon)$, comparable to the thickness of the plate. The temperature of the solid in these regions differs from the temperature of the corresponding fluid by amounts of order $\varepsilon^{1/5}$.

In the asymptotic limit $\alpha/\varepsilon^2 \to \infty$, the heat fluxes in the fluids remain finite and equation (40) implies $\theta_{wI} \to \theta_{wII}$, recovering the limit $\alpha \to 0$ of Subsection 3.2. The lengths of the regions where longitudinal conduction matters begin to increase when α/ε^2 becomes much larger than $\varepsilon^{-1/5}$.

In the opposite limit, $\alpha/\varepsilon^2 \to 0$, equation (40) implies that the heat fluxes in the fluids tend to zero and most of the temperature drop occurs in the solid: $\theta_{wI} \to 1$ and $\theta_{wII} \to 0$, except in small regions near the edges. Outside of these regions, the solid and fluid variables are of the form

$$\theta_w = z + \frac{1}{2} + \left(\frac{\alpha}{\varepsilon^2}\right)^{4/5}\theta_{wI} + O\left[\left(\frac{\alpha}{\varepsilon^2}\right)^{8/5}\right] \quad (41)$$

and, to leading order,

$$\tilde{f}_I = \left(\frac{\alpha}{\varepsilon^2}\right)^{1/5}\tilde{g}\left[\left(\frac{\alpha}{\varepsilon^2}\right)^{1/5}\tilde{\eta}_I, Pr_I\right]$$

$$\tilde{\theta}_I = \left(\frac{\alpha}{\varepsilon^2}\right)^{4/5}\tilde{\phi}\left[\left(\frac{\alpha}{\varepsilon^2}\right)^{1/5}\tilde{\eta}_I, Pr_I\right] \quad (42)$$

and

$$\tilde{f}_{II} = \left(\frac{\alpha\beta}{\varepsilon^2}\right)^{1/5}\tilde{g}\left[\left(\frac{\alpha\beta}{\varepsilon^2}\right)^{1/5}\tilde{\eta}_{II}, Pr_{II}\right]$$

$$\tilde{\theta}_{II} = \left(\frac{\alpha\beta}{\varepsilon^2}\right)^{4/5}\tilde{\phi}\left[\left(\frac{\alpha\beta}{\varepsilon^2}\right)^{1/5}\tilde{\eta}_{II}, Pr_{II}\right], \quad (43)$$

where $\tilde{g}(\xi, Pr)$ and $\tilde{\phi}(\xi, Pr)$ are the solution of the classical problem of a boundary layer with a constant heat flux at the wall ($d\tilde{\phi}/d\xi|_0 = -1$), which can be found elsewhere [10]. In particular,

$$\tilde{\phi}(0, Pr) = \tilde{G}(Pr) \equiv \left(\frac{4 + 9Pr^{1/2} + 10Pr}{Pr}\right)^{1/5}. \quad (44)$$

To this order, the nondimensional plate temperature is

$$\theta_w = z + \frac{1}{2} - \left(\frac{\alpha}{\varepsilon^2}\right)^{4/5}[\tilde{G}(Pr_I)\chi^{1/5}(z+\tfrac{1}{2}) + \beta^{4/5}\tilde{G}(Pr_{II})(1-\chi)^{1/5}(z-\tfrac{1}{2})] \quad (45)$$

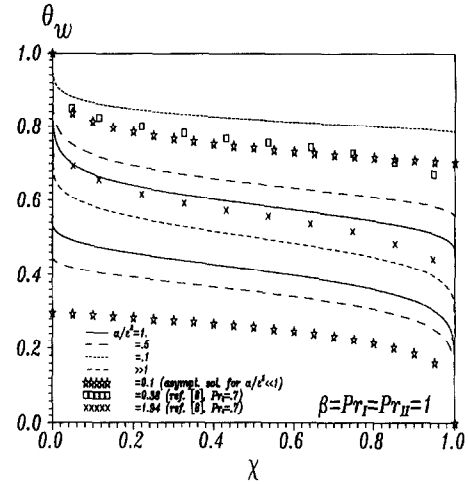

Fig. 6. Nondimensional temperature distributions at both surfaces of the plate from the numerical solution and from the two-term asymptotic solution for small values of α/ε^2. Upper curves correspond to the side facing the hot fluid. Results obtained in ref. [8] are also plotted.

and, evaluating the heat flux across the solid, $q = (\lambda_w \Delta T/h)\partial\theta_w/\partial z$, with this expression, the overall Nusselt number is

$$\overline{Nu} = \frac{\alpha Ra_I^{1/4}}{\varepsilon^2}\left[1 - \frac{5}{6}\left(\frac{\alpha}{\varepsilon^2}\right)^{4/5}(\tilde{G}(Pr_I) + \beta^{4/5}\tilde{G}(Pr_{II}))\right]. \quad (46)$$

Notice that, since $\alpha Ra_I^{1/4}/\varepsilon^2 = (\lambda_w/\lambda_I)/\varepsilon$, this Nusselt number does not depend on the Rayleigh number to leading order.

The distributions of θ_{wI}, θ_{wII} resulting from the numerical solution of the problem are plotted in Fig. 6 for several values of α/ε^2. The two-term asymptotic solution (45) is also plotted for $\alpha/\varepsilon^2 = 0.1$ in order to compare with the numerical results. The discrepancies are significant for values of $\alpha/\varepsilon^2 > 0.1$, and a third term would be needed in the asymptotic expansion to obtain a better approximation. Results for the limit $\alpha/\varepsilon^2 \to \infty$ are also included in Fig. 6, as well as a couple of points corresponding to the numerical results of ref. [8]. Figure 7 shows the overall reduced Nusselt number, $\overline{Nu}/Ra_I^{1/4}$, as a function of α/ε^2 for two different values of β. Both the numerical and the two-term asymptotic solution (46) are plotted. Again the agreement is good for values of $\alpha/\varepsilon^2 < 0.1$.

Finally, we note that the boundary layer approximation breaks down when α/ε^2 becomes of order $Ra_i^{-5/4}$, giving way to another regime in which the motion of the fluids occurs in regions of characteristic size L. For still smaller values of α/ε^2, this motion ceases to be relevant to the heat transfer, which occurs purely by conduction.

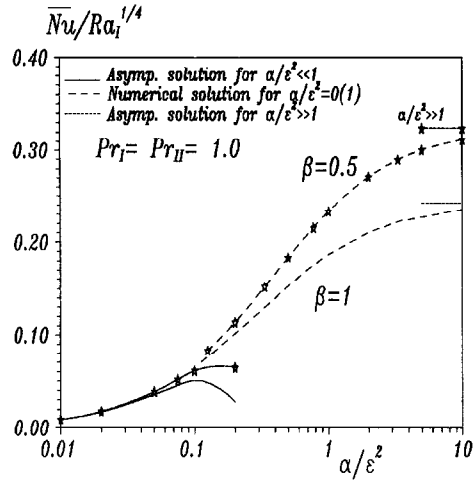

Fig. 7. Overall reduced Nusselt number, $\overline{Nu}/Ra_l^{1/4}$, as a function of α/ε^2, for $\beta = 0.5$ and 1. Results from the numerical solution (dashed curves) and from the asymptotic solutions for small and large α/ε^2.

5. EXAMPLE

An overview of the overall reduced Nusselt number as a function of α for $\varepsilon = 0.1$ is presented in Fig. 8 for two different values of β, ($\beta = 0.5$ and 1). This figure covers all the possible values of α and demonstrates the validity of the asymptotic limits we have analyzed. The results for different values of β coincide in the pure conduction regime (for very small values of α, such that $\alpha \ll \varepsilon^2$), and begin to separate when the effect of the natural convection becomes important, reaching higher values of the reduced Nusselt numbers for smaller values of β. The two-term asymptotic solution for $\alpha/\varepsilon^2 \ll 1$ is applicable up to $\alpha/\varepsilon^2 \simeq 0.001$, and the numerical solution for α/ε^2 of order unity, which does not include the effect of longitudinal heat conduction, covers all the parametric space up to $\alpha \simeq 0.1$. For comparison, we have included in Fig. 8 the result of ref. [6] for $\beta = 1$ and $Pr_i = 0.7$. If the effect of the slightly lower Prandtl number were corrected, this point would shift upwards approaching the dashed curve. The numerical solutions obtained in Section 4 for $\alpha/\varepsilon^2 = O(1)$ and in Section 3 for $\alpha = O(1)$ meet with each other in a fairly smooth way for α about 0.1. It is here that the effect of longitudinal heat conduction first enters the solution, and also where the reduced Nusselt number reaches its maximum. This maximum is close to the value found in Section 3.2 for $\varepsilon \to 0$.

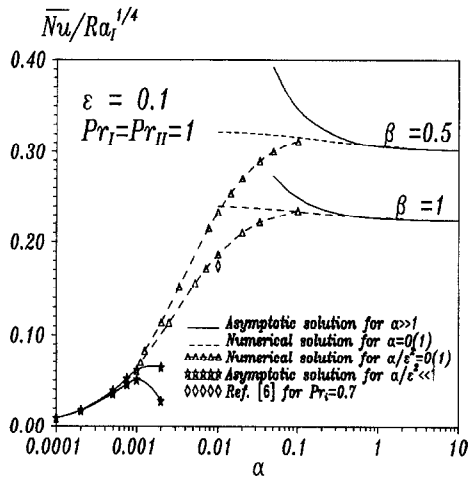

Fig. 8. General view of the overall reduced Nusselt number, $\overline{Nu}/Ra_l^{1/4}$, as a function of α, for $\beta = 0.5$ and 1, and $\varepsilon = 0.1$, obtained from the numerical and the asymptotic solutions.

By way of illustration, let us compare briefly these results with the experimental results of Sakakibara *et al.* ([8]). In their experiments, two expanses of air at temperatures $T_{1,\infty} = 302.7$ K and $T_{II,\infty} = 292.5$ K are separated by a plate 20 cm high and 2 cm wide. With these data, the Rayleigh number is $Ra_l = 7.455 \times 10^6$ and the values of ε and β are 0.1 and 1, respectively. The computed values of α are $\alpha = 8.8$ for an aluminium plate and $\alpha = 0.0796$ ($\alpha/\varepsilon^2 = 7.96$) for a Pyrex glass. In the first case, the relatively large value of α indicates that the non-dimensional wall temperature is very close to 0.5 and the longitudinal heat conduction is extremely important. The second case is at the border of the two cases analyzed in the present work, and the longitudinal heat conduction is not important. The experimental temperature profiles corresponding to this case have been transformed to our variables η_i and included in Fig. 3. The small discrepancies between the numerical computations and these experimental results can be attributed to two different causes. Firstly, the slightly different values of the Prandtl numbers (0.71 vs 1) and of α are no doubt responsible for the boundary layer appearing thinner in the computations than in the experiment. Secondly, the temperature drop across the plate is not entirely negligible in this experiment (nor does our analysis predict otherwise), whereas this effect was not included in the computations of Section 3. This is the reason for the discrepancies of the point on the right side of the plate in the profile for $\chi = 0.25$ and of the point on the left side in the profile for $\chi = 0.75$. An idea of the magnitude of the temperature difference between the two sides of the plate can be obtained from the evolution of the couples of curves in Fig. 6 for the three values of α/ε^2 displayed. The temperature difference should be small for $\alpha/\varepsilon^2 = 7.96$, according to these results, but still of the order of the discrepancies in Fig. 3. Thus, overall, we conclude that the comparison is favorable. Regrettably, no value of the Nusselt number appears in ref. [8], preventing direct comparison for this important quantity.

6. CONCLUSIONS

In this paper we have studied analytically and numerically the conjugated heat transfer across a wall separating two fluids at different temperatures. For

large Rayleigh numbers, this problem depends on five nondimensional parameters: α, β, ε and Pr_i. All of our results correspond to the asymptotic limit $\varepsilon \to 0$. Guided by the order of magnitude analysis of Section 2, we have discussed separately the case in which α remains finite as ε tends to zero and the case in which α/ε^2 remains finite.

In Section 3 we have formulated and numerically solved the problem for the first of these cases. In addition to obtaining the numerical solution, we have analyzed the asymptotic limits of large and small α. In the high α limit, the longitudinal heat conduction is extremely important in the plate and must be retained, whereas the temperature variation across the plate is very small and can be neglected (which does not mean, of course, that the transversal temperature gradient is negligible; it is important and is always accounted for in the analysis). This transversal temperature variation grows when α decreases, becoming of order $T_{I\infty} - T_{II\infty}$ for α of order ε^2. The limit $\alpha \to \infty$ is regular, and the asymptotic solution is sought as an expansion in powers of α^{-1}. Comparing this asymptotic solution with our numerical results and with those previously published in the literature, we find that a two-term expansion already gives very good results for values of α as small as 0.5. The influence of β, which takes values from 0 to ∞, and of the Prandtl numbers are explicitly shown in our asymptotic solution [see equations (35), (36) and the Appendix]. For very large values of β, the problem reduces to that of a uniform plate temperature, equal to the temperature $T_{I\infty}$ of the hot fluid at the left of the plate. In the opposite limit of very small values of β, the temperature of the plate takes the value $T_{II\infty}$ of the cold fluid at the right. We have given particular attention to the case $\beta = 1$, which includes the situation in which the fluids at both sides of the plate are the same.

The limit $\alpha \to 0$ is analyzed in Section 3.2. In this limit, the effect of the longitudinal heat conduction is very small and can be neglected except in small regions that appear around the edges of the plate in order to satisfy the adiabatic boundary conditions. The solutions in these regions are complex and are omitted here, but they have only a local effect. The overall Nusselt number in this asymptotic limit is the maximum attainable for given values of β and the Prandtl numbers.

The case of α/ε^2 finite as $\varepsilon \to 0$ has been discussed in Section 4. Numerical solutions of the corresponding problem have been obtained for $\alpha/\varepsilon^2 = O(1)$, whereas the mathematical problem for $\alpha/\varepsilon^2 \gg 1$ is seen to coincide with that of Section 3.2. The singular limiting case $\alpha/\varepsilon^2 \ll 1$ has been also analyzed, working out a two-term asymptotic expansion. In this limit we obtain good qualitative agreement with our numerical results and with those of refs [6] and [8], and probably a third term in the expansions would bring the asymptotic results to quantitative agreement.

The full parametric dependence has been presented in all the asymptotic limits analyzed. The overall nondimensional heat transfer rates are obtained both from the numerical and from the asymptotic solutions, when applicable. For large values of α/ε^2, the overall Nusselt number increases with decreasing α and does not depend on ε, while, for values of α/ε^2 of order unity, the overall Nusselt number decreases with α at ε constant. From this, we conclude that the overall Nusselt number is maximum for a finite value of α verifying $\varepsilon^2 \ll \alpha \ll 1$.

Acknowledgements—The work of C.T. and F.M. has been supported by a grant of DGAPA, UNAM, IN107795. F.J.H. acknowledges partial support by the Spanish DGI-CYT through grant PB92-1075.

REFERENCES

1. M. D. Kelleher and K. T. Yang, A steady conjugate transfer problem with conduction and free convection, *Appl. Sci. Res.* **17,** 249–269 (1967).
2. G. S. H. Lock and J. C. Gunn, Laminar free convection from a downward-projecting fin, *J. Heat Transfer* **90,** 63–70 (1968).
3. G. S. H. Lock and R. S. Ko, Coupling through a wall between two free convection systems, *Int. J. Heat Mass Transfer* **16,** 2087–2096 (1973).
4. R. Anderson and A. Bejan, Natural convection on both sides of a vertical wall separating fluids at different temperatures, *J. Heat Transfer* **102,** 630–635 (1980).
5. R. Anderson and A. Bejan, Heat transfer through single and double vertical walls in natural convection: theory and experiment, *Int. J. Heat Mass Transfer* **24,** 1611–1620 (1981).
6. R. Viskanta and O. W. Lankford, Coupling of heat transfer between two natural convection systems separated by a vertical wall, *Int. J. Heat Mass Transfer* **24,** 1171–1177 (1981).
7. S. W. Churchill and H. Ozoe, A correlation for laminar free convection from a vertical plane, *J. Heat Transfer* **C95,** 540–541 (1973).
8. M. Sakakibara, H. Amaya, S. Mori and A. Tanimoto, Conjugate heat transfer between two natural convections separated by a vertical plane, *Int. J. Heat Mass Transfer* **35,** 2289–2297 (1992).
9. J. Córdova and C. Treviño, Effects of longitudinal heat conduction of a vertical thin plate in a natural convective cooling process, *Wärme Stoffübertragung* **29,** 195–204 (1994).
10. W. M. Kays and M. E. Crawford, *Convective Heat and Mass Transfer* (2nd Edn). McGraw-Hill, New York (1980).

APPENDIX

The solution of equations (18), (21)–(24), (27) and (28) for $\alpha \gg 1$ can be written in the form ($i = \mathrm{I}, \mathrm{II}$)

$$\theta_w = \sum_{j=0}^{\infty} \frac{1}{\alpha^j} \theta_{wj}(\chi), \quad \theta_i = \sum_{j=0}^{\infty} \frac{1}{\alpha^j} \theta_{ij}(\chi, \eta_i), \quad f_i = \sum_{j=0}^{\infty} \frac{1}{\alpha^j} f_{ij}(\chi, \eta_i), \tag{A1}$$

where the leading terms of these series are given by equations (35), (29) and (30). In this Appendix we compute the second terms.

First, carrying equations (29), (30) and (A1) into equation (27), collecting terms of order unity, and integrating twice the resulting equation, we find

$$\theta_{w1} = \tfrac{16}{21} G_I (1-\theta_{w0})^{5/4}((1-\chi)^{7/4} + \tfrac{7}{4}\chi - \chi^{7/4} + C_1)$$
$$= \tfrac{16}{21} G_I (1-\theta_{w0})^{5/4}\left(1 + C_1 - \chi^{7/4} + \sum_{n=2}^{N} a_n \chi^n\right)$$
$$= \tfrac{16}{21} G_I (1-\theta_{w0})^{5/4}\left(C_1 + \tfrac{3}{4} + \chi_{II}^{7/4} - \sum_{n=2}^{N} a_n \chi_{II}^n\right) \quad \text{(A2)}$$

where C_1 is an unknown constant and, for convenience, we have written θ_{w1} in two alternative forms as power series of χ_I and of χ_{II}. Here a_n are the coefficients of the binomial expansion of $(1-\chi)^{7/4}$.

Second, as can be easily verified by substituting equation (A1) into equations (21)–(24) and (28) and collecting terms proportional to α^{-1}, the quantities θ_{i1} and f_{i1}, $(i = I, II)$ satisfy linear problems whose solutions for a surface temperature of the form $\theta_{w1} = A\chi_i^n$ would be

$$f_{I1} = A\chi_I^n (1-\theta_{w0})^{-3/4} \boldsymbol{g}_1[(1-\theta_{w0})^{1/4}\eta_I, Pr_I],$$
$$\theta_{I1} = -A\chi_I^n \phi_1[(1-\theta_{w0})^{1/4}\eta_I, Pr_I], \quad \text{(A3)}$$

and

$$f_{III} = A\chi_{II}^n \theta_{w0}^{3/4} \boldsymbol{g}_1[\theta_{w0}^{1/4}\eta_{II}, Pr_{II}], \quad \theta_{III} = A\chi_{II}^n \phi_1[\theta_{w0}^{1/4}\eta_{II}, Pr_{II}], \quad \text{(A4)}$$

with $\boldsymbol{g}_1(\xi, Pr)$ and $\phi_1(\xi, Pr)$ satisfying

$$\frac{d^3\boldsymbol{g}_1}{d\xi^3} + \phi_1 + \frac{1}{Pr}\left\{-\frac{d\boldsymbol{g}}{d\xi}\frac{d\boldsymbol{g}_1}{d\xi} + \frac{3}{4}\frac{d^2\boldsymbol{g}}{d\xi^2}\boldsymbol{g}_1 + \frac{3}{4}\boldsymbol{g}\frac{d^2\boldsymbol{g}_1}{d\xi^2} - n\left[\frac{d\boldsymbol{g}}{d\xi}\frac{d\boldsymbol{g}_1}{d\xi} - \frac{d^2\boldsymbol{g}}{d\xi^2}\boldsymbol{g}_1\right]\right\} = 0, \quad \text{(A5)}$$

$$\frac{d^2\phi_1}{d\xi^2} + \frac{3}{4}\boldsymbol{g}\frac{d\phi_1}{d\xi} + \frac{3}{4}\frac{d\phi}{d\xi}\boldsymbol{g}_1 - n\left[\frac{d\boldsymbol{g}}{d\xi}\phi_1 - \frac{d\phi}{d\xi}\boldsymbol{g}_1\right] = 0, \quad \text{(A6)}$$

$$\boldsymbol{g}_1 = \frac{d\boldsymbol{g}_1}{d\xi} = \phi_1 - 1 = 0 \quad \text{at} \quad \xi = 0$$
$$\text{and} \quad \frac{d\boldsymbol{g}_1}{d\xi} = \phi_1 = 0 \quad \text{for} \quad \xi \to \infty. \quad \text{(A7)}$$

The functions $G_1(n, Pr) \equiv -d\phi_1/d\xi|_{\xi=0}$ obtained from the solution of equations (A5)–(A7) are given in ref. [9].

Then, taking advantage of equations (A3) and (A4) and of the series expansions (A2) for θ_{w1}, and applying the superposition principle to the linear problems for f_{i1} and θ_{i1}, we immediately obtain

$$\left.\frac{\partial\theta_{I1}}{\partial\eta_I}\right|_{\eta_I=0} = \tfrac{16}{21} G_I (1-\theta_{w0})^{3/2} \times\left((1+C_1)G_1(0, Pr_I) - G_1(\tfrac{7}{4}, Pr_I)\chi^{7/4} + \sum_{n=2}^{N} a_n G_1(n, Pr_I)\chi^n\right), \quad \text{(A8)}$$

and

$$\left.\frac{\partial\theta_{III}}{\partial\eta_{II}}\right|_{\eta_{II}=0} = -\tfrac{16}{21} G_I (1-\theta_{w0})^{1/4}\theta_{w0}^{5/4} \times\left((C_1 + \tfrac{3}{4})G_1(0, Pr_{II}) + G_1(\tfrac{7}{4}, Pr_{II})\chi_{II}^{7/4} - \sum_{n=2}^{N} a_n G_1(n, Pr_{II})\chi_{II}^n\right). \quad \text{(A9)}$$

Finally

$$C_1 = \frac{H_N(Pr_I, Pr_{II})}{H_D(Pr_I, Pr_{II})}, \quad \text{(A10)}$$

is obtained by carrying equations (A8) and (A9) into equation (27) and integrating this equation over χ with the boundary conditions (18). Here,

$$H_N = \left(\frac{\beta G_I}{G_{II}}\right)^{1/5}\left(-\tfrac{3}{4}G_{1II}(0) - \tfrac{3}{10}G_{1II}(\tfrac{7}{4}) + \sum_{n=2}^{N}\frac{a_n G_{1II}(n)}{(\frac{4}{3}n+1)}\right) - G_{1I}(0) + \tfrac{3}{10}G_{1I}(\tfrac{7}{4}) - \sum_{n=2}^{N}\frac{a_n G_{1I}(n)}{(\frac{4}{3}n+1)}, \quad \text{(A11)}$$

$$H_D = G_{1I}(0) + \left(\frac{\beta G_I}{G_{II}}\right)^{1/5} G_{1II}(0), \quad \text{(A12)}$$

and we have used the notation $G_{1i}(n) = G_1(n, Pr_i)$. Notice that both H_N and H_D are zero for the particular case in which the fluids at the two sides of the plate are the same. In this case symmetry implies $\theta_{w1}(1/2) = 0$ and $C_1 = -7/8$.

The factor $F(Pr_I, Pr_{II}, \beta)$ in the correction equation (37) to the Nusselt number equation (36) can now be evaluated as

$$F = \frac{16}{21}\frac{\dfrac{G_{II}}{G_I}}{\left(\left(\dfrac{G_{II}}{G_I}\right)^{4/5} + \beta^{4/5}\right)^{5/4}}\left((1+C_1)G_{1II}(0) - \tfrac{3}{10}G_{1II}(\tfrac{7}{4}) + \sum_{n=2}^{\infty}\frac{a_n G_{1II}(n)}{\frac{4}{3}n+1}\right). \quad \text{(A13)}$$